

Photo-induced flexible semiconductor CdSe/CdS quantum rods alignment

Wanlong Zhang^{1,†}, Julian Schneider³, Maksym F. Prodanov², Valerii V. Vashchenko², Andrey L. Rogach³, Xiaocong Yuan¹, and Abhishek K. Srivastava^{2,†}

¹Nanophotonics Research Center, Institute of Microscale Optoelectronics, Shenzhen University, Shenzhen 518060, China

²State Key Laboratory of Advanced Displays and Optoelectronics Technologies, Department of Electronic & Computer Engineering, Hong Kong University of Science and Technology, Hong Kong SAR, China

³Department of Materials Science and Engineering and Centre for Functional Photonics (CFP), City University of Hong Kong, Hong Kong SAR, China

Abstract: The anisotropic absorption and emission from semiconductor CdSe/CdS quantum rods (QRs) provide extra benefits among other photoluminescence nanocrystals. Using photo-induced alignment technique, the QRs can be oriented in liquid crystal polymer matrix at a large scale. In this article, a 2D Dammann grating pattern, within “SKL” characters domains aligned QRs in composite film, was fabricated by multi-step photo exposure using several photo masks, and a continuous geometric lens profile pattern aligned QRs was realized by the single step polarization converting holographic irradiation method. Both polarized optical microscope and fluorescence microscope are employed to determine the liquid crystal director profiles and QRs anisotropic excitation properties. We have been able to orient the QRs in fine binary and continuous patterns that confirms the strong quantum rod aligning ability of the proposed method. Thus, the proposed approach paves a way for photo-induced flexible QRs alignments to provide a highly specific and difficult-to-replicate security application at a large scale.

Key words: quantum rods; photo alignment; liquid crystal; flexible alignment; polarized emission

Citation: W L Zhang, J Schneider, M F Prodanov, V V Vashchenko, A L Rogach, X C Yuan, and A K Srivastava, Photo-induced flexible semiconductor CdSe/CdS quantum rods alignment[J]. *J. Semicond.*, 2023, 44(9), 092605. <https://doi.org/10.1088/1674-4926/44/9/092605>

1. Introduction

Semiconductor quantum materials, such as quantum dots^[1] and perovskite nanocrystals^[2], exhibit unique photoluminescence with high quantum yield and luminescence properties^[3, 4]. Owing to their tunable fluorescent properties, narrow bandwidth emission and stable chemical properties, the quantum nanocrystals are used in modern displays for wide color gamut^[5–7]. For example, replacing both organic dyes and inorganic phosphors, the quantum nanocrystals work as color down-converters for blue light-emitting diodes (LEDs) backlight unit of liquid crystal displays (LCDs)^[8–13]. Other than 0D quantum dots, both 1D quantum rods (QRs) and 2D nanoplatelets could offer an added advantage for LCDs due to the partially polarized absorption and emission properties^[14–17]. Among the above nanocrystals, the anisotropic optical properties in CdSe/CdS QRs, including an increased absorption and partially polarized emission along the long axis, when the aspect ratio of the shell exceeds 1.2 : 1^[14]. As the typical CdSe/CdS QRs, both dot-in-rods and rod-in-rods structured exhibit the additional anisotropy originating from the splitting of the exciton fine structure in the wurtzite CdSe core^[18]. According to the band-edge exciton fine structure, the room temperature emission from QRs is a

mixture of recombinations from the $|0^U\rangle$ state and from the degenerate $|\pm 1^L\rangle$, $|\pm 1^U\rangle$ states. The $|0^U\rangle$ state is associated with a linear 1D dipole that oscillates along the long axis of the rods and emits linearly polarized photons, while the $|\pm 1^L\rangle$ and $|\pm 1^U\rangle$ states can be seen as 2D dipoles, containing the oscillating around the core and along the shell, respectively. The 2D dipoles are also equivalent to 2 linear dipoles, oscillating perpendicularly and in quadrature into the plane perpendicular to the long axis of the QRs^[19–21]. The elongated shaper induces the level ordering and the oscillator strengths of the various transitions. In the excited state, the electron wavefunction from the CdSe core is able to extend into the conduction band of the CdS shell, and into the shell volume to create polarized emission^[15, 22–24]. Therefore, the degree of the polarization for the total emission strongly depends on the relative oscillator strengths of two oscillators mutually oscillating in an orthogonal plane.

However, the proper processing is required for those anisotropic non-spherical nanocrystals to be assembled with a high degree of orientational order, so as to gain the benefits of the linearly polarized emission as an ensemble. Many techniques have been explored in this regard, including evaporation-mediated assembly^[25], magnetic field-assisted assembly^[26], electric field-assisted assembly^[27–29], template-assisted assembly^[30], mechanical rubbing^[31], liquid crystal self-alignment^[32], Langmuir-Blodgett deposition^[33], electrospinning^[34], stretching of polymer matrix^[22]. Among all above approaches, the photo-induced CdSe/CdS QRs alignment was

Correspondence to: W L Zhang, zwl@szu.edu.cn; A K Srivastava, eeabhishek@ust.hk

Received 14 AUGUST 2023; Revised 13 SEPTEMBER 2023.

©2023 Chinese Institute of Electronics

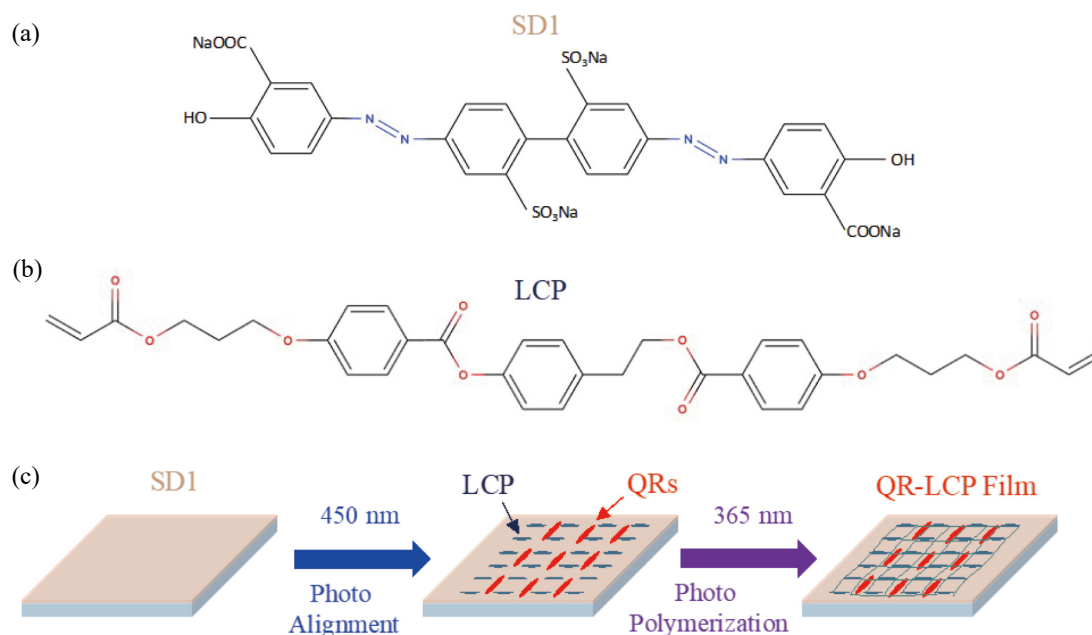


Fig. 1. (Color online) Photo-induced QRs alignment. Chemical structure of (a) SD1 and (b) LCP. (c) Process flow for unidirectional QRs alignment.

developed, offering high spatial alignment resolution as well as facilitating QRs aligning in liquid crystal polymer (LCP) networks^[35–45]. When exposed by a 450 nm polarized light, the azo-dye molecules SD1, as shown in Fig. 1(a), are reoriented from the initial position to the direction orthogonal to the E-vector of the exposure light for minimizing absorption due to the transition dipole moments of the molecules^[46]. The photo-aligned SD1 layer transfers the anchoring torque to the LCP molecules, as shown in Fig. 1(b), and aligns them in a direction parallel to the easy axis^[47, 48]. Simultaneously, due to the repulsive intermolecular forces between the QRs passivating ligands (alkylphosphonic acids) and LCP molecules, which exert counter-torque on QRs, QRs are aligned perpendicular to the easy axis of the SD1 molecules. The QRs ligands, to minimize the bulk energy, try to fit in the monomer matrix like a comb, resulting a long range order to QRs alignment^[35, 42, 43].

Traditional security films are often made of polymer materials and have features such as holograms, watermarks, and micro-text to prevent counterfeiting. In addition to these conventional features, the anisotropic absorption and emission properties of QRs offer a unique and advanced approach to enhancing the security of documents. In this paper, we demonstrate a flexible CdSe/CdS QRs alignment in QRs-LCP composite films, facilitated by photo-induced alignment technique. With the unique reorientation property of SD1, a 2D Damman grating pattern within “SKL” characters domains aligned QRs-LCP composite film was fabricated by multi-step polarized irradiation using several shadow-masks. The secured information “SKL” presents watermark under ambient light, red color emission under ultra-violet or blue light, as well as diffraction hologram with incident beam, providing a highly specific and difficult-to-replicate security feature.

To further present the flexibility of photo-induced alignment technique, single step polarization holographic irradiation for Pancharactnam Berry optical lens pattern aligned QRs-LCP composite film was exhibited to achieve the in-plane continuously varying alignment axis of QRs. The polar-

ized fluorescence microscopy (FM) images confirm the flexible QRs alignment in the composite films, indicating the potential applications of these uniquely aligned QR films in security, displays and photonics areas.

2. Experimental results

2.1. Unidirectional photo-induced QRs alignment

The unidirectional photo-induced QRs alignment process flow is shown in Fig. 1(c). A solution of SD1 in N,N-Dimethylmethanamide (DMF) is spin coated on a glass substrate, which is baked at 100 °C for 5 min to remove excessive solvent. The thin film of SD1 is then exposed to linearly polarized blue (450 nm) light, offering an almost zero pretilt angle ($<0.2^\circ$) and high anchoring energy ($\sim 10^{-3}$ J/m²)^[47]. The solution of highly emissive semiconductor QRs mixed in the LCP matrix is deposited on the SD1 layer by spin coating. With evaporating majority part of the solvent, the LCP molecules are highly ordering aligned following the easy axis of SD1 layer. At the same time, the QRs in the mixture are oriented to the perpendicular direction of LCP alignment, due to the repulsive force between the QRs ligands and LCP molecules. To solidify the obtained composite layer and freeze the alignment of QRs, the films are photo polymerized by high power UV light with vacuum, which speeds up the polymerization process as well as reduces the defects of re-orientation of QRs and LCP due to the unpolarized UV light source. The resulting films should show good stability, high transparency and birefringence under cross polarizer.

To examine the long-range orientation of the QRs in the composite film, optical characterization by polarized photo spectrometer is employed as a standard characterization technique. The polarization ratio, or degree of polarization of the QRs emission excited by a 450 nm laser can be measured by rotating the polarizer in front of the spectrometer. The polarization azimuth of the laser is set in line with the alignment direction of the QRs, to achieve the maximum absorption and emission^[37, 38].

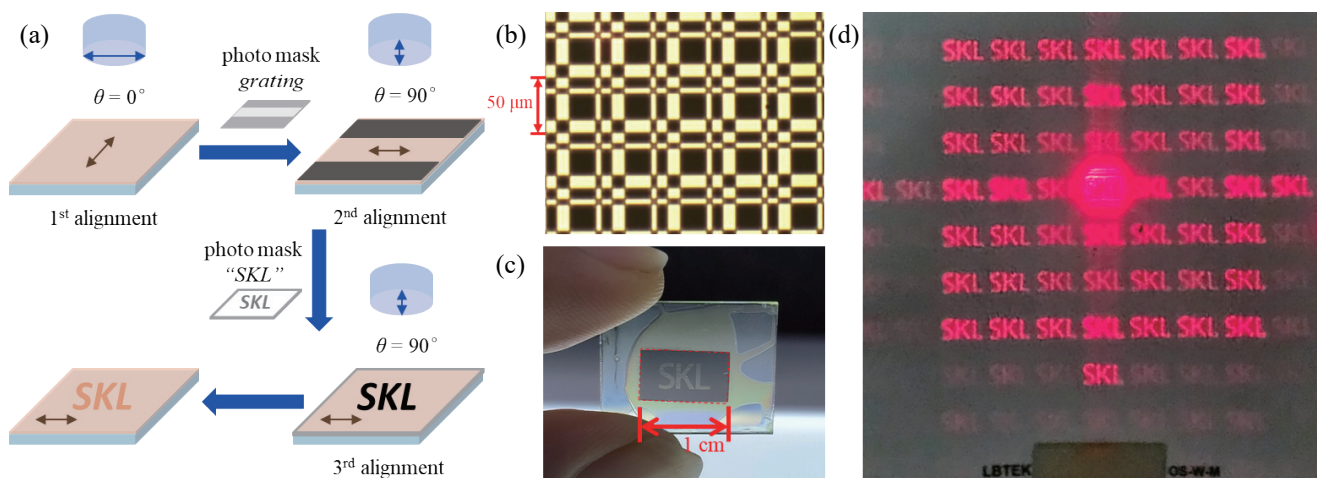


Fig. 2. (Color online) 2D Dammann pattern QRs alignment. (a) Process flow of multi domain photo alignment. (b) Photo mask of Dammann grating. (c) QRs-LCP composite film of Dammann pattern within “SKL” characters. (d) Diffraction pattern of “SKL” characters.

2.2. 2D Dammann pattern QRs alignment

Dammann gratings, first proposed by Dammann and Gortler in 1971, are specially designed binary phase ($0, \pi$) gratings that can create a diffraction pattern where the intensities of the diffracted spots are equal in some orders^[49]. The Dammann gratings have been proposed for usage in lots of interesting applications, such as laser beam summation, optical digital computing, optical interconnections, 3D lattice structures generation, 3D optical imaging, etc. Here, the QRs are aligned along Dammann pattern with special characters for potential security applications.

The re-writability of SD1 allows us to change the orientation of the easy axis several times by sequential energy exposures. This unique re-orientation property provides an opportunity to precisely modify the pre-alignment and realize the multi-alignment domains on the same substrate by multi-step exposures^[36, 47]. This advantage offers a possibility to align QRs in LCP composite films with several domains by using shadow masks.

Fig. 2(a) introduces the patterned photo-alignment fabrication process flow using multi exposure steps. The QRs-LCP mixture, coated on the top of these SD1 coated substrate, follows the alignment induced by the SD1 and the composite film can be polymerized afterwards. The SD1 layer is firstly aligned along the long side of the substrate by illumination it with the linearly polarized light (here denoted as $\theta = 0^\circ$, $\lambda = 450$ nm). Subsequent exposure with polarized light of orthogonal polarization azimuth (here $\theta = 90^\circ$) re-orientates the easy axis of SD1 by restricting the exposed area through a 7×7 Dammann grating photo-mask, as shown in Fig. 2(b). Thereby inducing the orthogonal alignment direction in the two domains. Note that the difference of θ between the first and second exposure defines the mutual orientation of the easy axis within different alignment domains. To obtain the maximum contrast between adjacent domains we fixed the mutual angle between the two alignment easy axis at 90° . The 3rd alignment of the same polarization azimuth, covering another photomask of “SKL” characters, the area out of the characters is transparent for the 3rd exposure, whereas the area blocked by the characters maintains the Dammann grating pattern. The active area, enclosed by a red square, is shown in Fig. 2(c), while the area outside the square is filled

with unaligned QR-LCP film, resulting in a hazy appearance. After polymerization of the deposited QRs-LCP mixtures, the active area in Fig. 2(c) displays the hazy “SKL” characters due to the micro-grating domain structures. The area outside the “SKL” characters maintains a unidirectional alignment of QR-LCP, resulting in a clear and transparent appearance.

Fig. 2(d) shows the diffraction pattern of the Dammann grating, instead of normal diffraction pattern of dots from traditional gratings, the 7×7 “SKL” characters are equally distributed on the screen, presenting unique diffraction features of the composite film and indicating the potential usage for security application. Since the LCP film is not thick enough for half wave phase retardation of the laser beam, the diffractive zero order cannot be suppressed, leaving a strong zero order intensity at the center of the diffraction pattern on the screen.

Other than diffraction pattern, the microscopic patterns (see Fig. 3), are also security features for the application. In the bright field, the QRs-LCP composite film between cross polarizers, the 2-domain LCP alignment can be observed due to the birefringence of the materials, as shown in Fig. 3(a). With the fluorescence mode, the excitation beam passes through the polarizer to form a linearly polarized beam. Due to the anisotropic absorption of the aligned QRs in composite film, the positive and negative images are obtained with the polarization azimuth perpendicular and parallel to the uniform alignment direction, are shown in Figs. 3(b) and 3(c), respectively. This anisotropic absorption and emission properties are critical special for the QRs only, increasing the unique security features.

2.3. Continuous pattern QRs alignment

In our previous work, we achieved $2 \mu\text{m}$ of the finest domain sizes of 2D QRs pattern alignment, which was proven by the FM^[36]. Since the direct exposure with photo mask is still limited by the resolution of masks, divergence of exposure light source, gap between mask and sample, etc., it is extremely difficult to further scale down the domain size. Apart from the orthogonal pattern alignment structure and the multi-step exposures, here we present the polarization converting hologram (PCH) for continuous QRs alignment in a single step only. The PCH encodes the macroscopic topology of

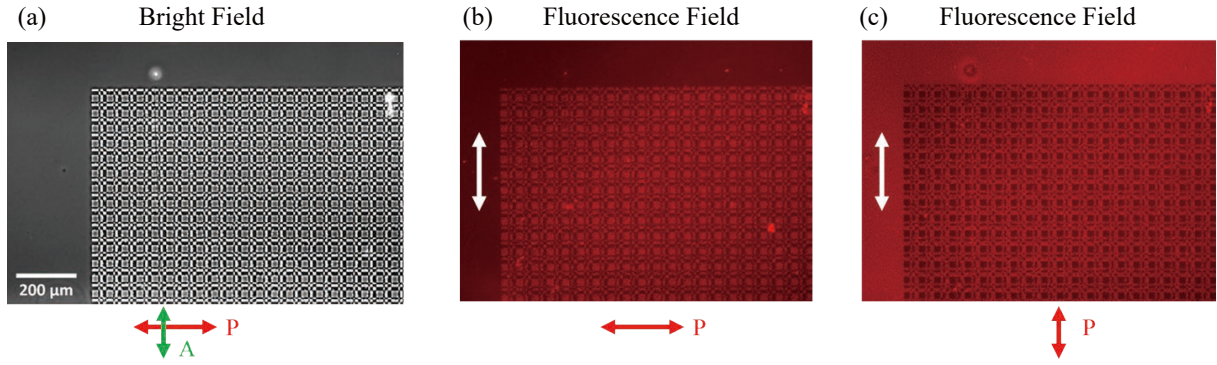


Fig. 3. (Color online) Dammann grating pattern under fluorescence microscope. (a) Bright field image between cross polarizes. Fluorescence field images with polarization azimuth (b) perpendicular and (c) parallel to uniform alignment direction (white arrow) of QRs in the composite film, respectively.

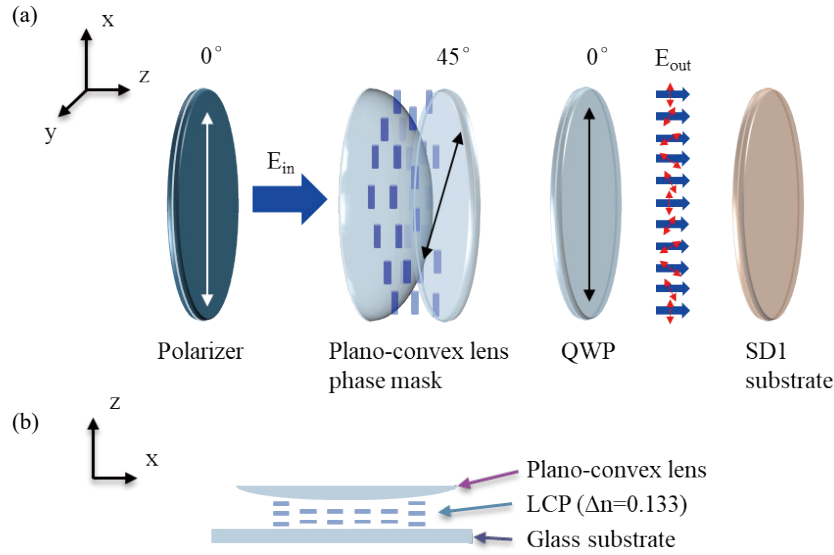


Fig. 4. (Color online) Principle of polarization converting hologram (PCH). (a) Optical scheme of PCH exposure. (b) Cross-section scheme of the plano-convex lens phase mask.

an optical element (i.e. lens) and converts this topological structure into continuously polarization azimuth distribution, projecting onto the SD1 substrate from the optical setup. The elegance of PCH is the fabricated holographic lens alignment profile with extremely high resolution (several of orders of magnitude higher than direct exposure), and can be established in a single step exposure.

The optical setup for PCH exposure is shown in Fig. 4(a), which comprises of a polarizer, a spatial retarder, and a quarter wave plate (QWP) after it. In this paper, the spatial retarder is described as a plano-convex lens phase mask, realized by sandwiching a layer of LCP in between a plano-convex lens and a glass substrate, forming a liquid crystal cell with lens-like cell gap distribution, the cross-section is shown in Fig. 4(b). The cell gap d between the plano-convex lens and the glass substrate is given by

$$d(x, y) = d(r) = R \left(1 - \sqrt{1 - \frac{r^2}{R^2}} \right) \approx \frac{r^2}{2R}, \quad (1)$$

where $R = 75$ mm is the radius of the plano-convex lens curvature, and r is the radial distance from the origin. Since R is much greater than the thickness of the sandwiched LCP

region, the separation distance d can be approximated by a parabola, i.e. $d(r) \propto r^2$.

Since the optical axis (LC alignment direction) of the plano-convex lens phase mask is orientated at 45° , with respect to the polarization azimuth of the linear polarizer as well as the fast axis of QWP are aligned along the transmission axis, denoted as 0° , the polarization azimuth distribution at the output plane can be calculated by Jones Matrix:

$$E_{\text{out}} = G_{\text{QWP}}(\theta) G_{\text{WP}}[\Gamma(r)] R(-\theta) E_{\text{in}} = i \begin{bmatrix} \cos\left(\frac{\Gamma(r)}{2}\right) \\ \sin\left(\frac{\Gamma(r)}{2}\right) \end{bmatrix}, \quad (2)$$

where $\Gamma(r) = 2\pi\Delta n d(r)/\lambda$ is the spatially varying retardation of the phase mask, $\Delta n = 0.133$ is the birefringence of LCP, $\lambda = 450$ nm is the wavelength of the exposure light. $R(\theta)$ and $R(-\theta)$ are the rotational matrix, $\theta = 45^\circ$ is the angle between polarization azimuth of the polarizer and the optical axis of the phase mask. $G_{\text{QWP}} = \begin{bmatrix} 1 & 0 \\ 0 & i \end{bmatrix}$ denotes the QWP with the fast axis align along the x -axis. $E_{\text{in}} = [1 \ 0]^T$ is the polarization azimuth of the incident light, which is along x -axis, too.

Thus, the Eq. (2) shows that after the light propagates through the PCH system, the polarization azimuth of the incident beam is rotated by an angle of $\Gamma(r)/2$, which is governed by the retardation of the phase mask. Using the expression from Eq. (1), the polarization azimuth's rotational angle distribution of the exposure light onto the SD1 alignment layer, $\varphi_R(x, y)$ is given by:

$$\varphi_R(x, y) = \frac{\Gamma(r)}{2} = \left(\frac{\pi \Delta n}{2R\lambda} \right) r^2. \quad (3)$$

Given that the exposure dose is sufficient, the orientation of SD1 molecules will be aligned perpendicular to the polarization azimuth of the exposure light. Since Eq. (1) is continuous parabolic function, resulting the orientation of the SD1 easy axis is continuously varying across the substrate. Moreover, the recorded alignment profile follows the parabolic separation cell gap of the spatial plano-convex lens phase retarder, thus the alignment resolution is dependent on the dimensions of the phase mask^[50].

With depositing the QRs-LCP mixtures, the directors of LCP molecules follow the directions perpendicular to the orientation of the exposure light polarization azimuth, which further induces the orientation of QRs will continuously follow the exposure light polarization azimuth distribution. Fig. 5(a) shows the QRs-LCP composite film under polarized optical microscope (POM), the LCP molecules (denoted in blue cylinders) are following the SD1 easy axis distribution, indicating the theoretically expected profile of a gradual decrease in grating pitch away from the center with smooth variations in transmittance level, plotted as dark line in Fig. 5(b), due to the birefringent property of LCP materials.

Fig. 5(c) presents the QRs emission under polarized excitation under FM. The QRs (denoted in yellow cylinders) are arranged perpendicular to the LCP direction. Since the oriented QRs offer not only polarized emission but also anisotropic absorption at the macroscopic scale, the emission intensity varies along with the angle between QRs and the excitation polarization azimuth^[38], resulting gradual bright and dark rings. The emission intensity profile of QRs through the center of the rings is also theoretically plotted as red line in Fig. 5(b), with corresponding position. The throughout green dash line is drawn as the reference position of each picture.

Moreover, the POM image in Fig. 5(a) and the FM image in Fig. 5(c) are of the same scale, however, the pitch of POM image is a half of that of FM image. It can be explained by the intensity profile of LCP under cross polarizer that, when the LC director locate at either parallel or perpendicular to the polarizer, the dark frame can be observed under POM, whereas the bright frame will be seen once the LC director is 45° to the polarizer. On the contrary, the emission intensity from the QRs in composite film observed under FM will be strictly following the angle between QRs and excitation polarization azimuth, resulting bright frame at 0° and dark frame at 90° to the polarizer, respectively. Fig. 5(b) clearly illustrates the relationship of these two intensity profiles.

3. Conclusion

In this paper, we have proposed and successfully demonstrated the flexibility of CdSe/CdS quantum rods alignment in

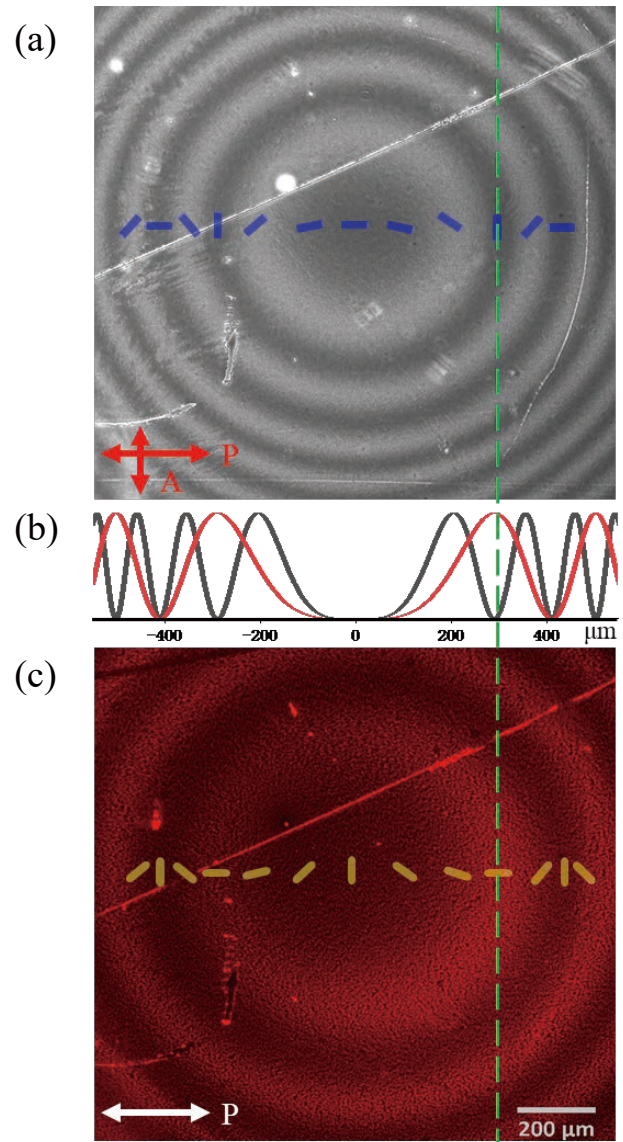


Fig. 5. (Color online) Continuously QRs-LCP alignment composite film under (a) polarized optical microscope, (c) fluorescence microscope with polarized excitation. (b) Theoretical intensity profiles through corresponding horizontal centers, respectively.

quantum rods-liquid crystal polymer composite films, facilitated by photo-induced alignment technique. A 2D Dammann grating pattern within "SKL" characters domains aligned quantum rods in composite film was fabricated by multi-step photo exposure along with several photo masks. With laser beam propagation through the Dammann grating, the 7×7 "SKL" characters are equally distributed on the screen, presenting unique diffraction features of the composite film. The FM is utilized to analyze the quantum rods pattern emission. In the bright field, the quantum rods-liquid crystal polymer composite film between cross polarizers, the 2-domain liquid crystal polymer alignment can be observed due to the birefringence of the materials. In the fluorescence mode, with the anisotropic absorption and emission of the aligned quantum rods in composite film, the positive and negative images excited by polarized light are obtained with the polarization azimuth perpendicular and parallel to the uniform alignment direction, respectively.

To further explore the aligning ability of quantum rods in

the composite system, the single step polarization converting hologram is introduced for continuous alignment of quantum rods. The plano-convex lens phase mask is applied to generate the continuous SD1 director distribution on the substrate, providing the geometric phase lens profile for quantum rods-liquid crystal polymer alignment in the composite film. The polarization optical microscope and fluorescent microscope are deployed to observe the intensity profiles. The pitch differences under different microscopes are observed due to the birefringent property of liquid crystal polymer and anisotropic emission of quantum rods. With recent development of quantum rods in liquid crystal polymer composite mixtures, the interaction between the quantum rods ligands and liquid crystal polymer molecules are improved for better compatibility^[39, 43], providing the potential use of flexible photo-induced quantum rods alignment in quantum rods-liquid crystal polymer composite films for security applications.

Acknowledgments

This work was supported by the Guangdong Major Project of Basic and Applied Basic Research (No. 2020B0301030009), the National Natural Science Foundation of China (Nos. 62005180, 61935013), the Zhejiang Lab Open Research Project (No. K2022MG0AB01), RGC of Hong Kong S. A. R. (No. 26202019), and the State Key Laboratory of Advanced Displays and Optoelectronics Technologies (HKUST) (No. ITC-PSKL12EG02).

References

- [1] Haus J W, Zhou H S, Honma I, et al. Quantum confinement in semiconductor heterostructure nanometer-size particles. *Phys Rev B*, 1993, 47, 1359
- [2] Huang H, Polavarapu L, Sichert J A, et al. Colloidal lead halide perovskite nanocrystals: Synthesis, optical properties and applications. *NPG Asia Mater*, 2016, 8, e328
- [3] Kim T H, Cho K S, Lee E K, et al. Full-colour quantum dot displays fabricated by transfer printing. *Nature Photon*, 2011, 5, 176
- [4] Wang K, Sun X W. Quantum-dot and quantum-rod displays—the next big wave. *Inf Disp*, 2016, 32, 6
- [5] Srivastava A K, Zhang W L, Schneider J, et al. Luminescent down-conversion semiconductor quantum dots and aligned quantum rods for liquid crystal displays. *Adv Sci*, 2019, 6, 1901345
- [6] Zhu R D, Luo Z Y, Chen H W, et al. Realizing Rec. 2020 color gamut with quantum dot displays. *Opt Express*, 2015, 23, 23680
- [7] Luo Z Y, Chen Y, Wu S T. Wide color gamut LCD with a quantum dot backlight. *Opt Express*, 2013, 21, 26269
- [8] Steckel J S, Ho J, Hamilton C, et al. Quantum dots: The ultimate down-conversion material for LCD displays. *Jnl Soc Info Display*, 2015, 23, 294
- [9] Chen H W, He J, Wu S T. Recent advances on quantum-dot-enhanced liquid-crystal displays. *IEEE J Sel Top Quantum Electron*, 2017, 23, 1
- [10] Zhou Q C, Bai Z L, Lu W G, et al. *In situ* fabrication of halide perovskite nanocrystal-embedded polymer composite films with enhanced photoluminescence for display backlights. *Adv Mater*, 2016, 28, 9163
- [11] Yoon H C, Lee H, Kang H, et al. Highly efficient wide-color-gamut QD-emissive LCDs using red and green perovskite core/shell QDs. *J Mater Chem C*, 2018, 6, 13023
- [12] Lu M, Zhang Y, Wang S X, et al. Metal halide perovskite light-emitting devices: Promising technology for next-generation displays. *Adv Funct Materials*, 2019, 29, 1902008
- [13] Gao Y Y, Prodanov M F, Kang C B, et al. Stable bright perovskite nanoparticle thin porous films for color enhancement in modern liquid crystal displays. *Nanoscale*, 2021, 13, 6400
- [14] Hu J T, Li L S, Yang W D, et al. Linearly polarized emission from colloidal semiconductor quantum rods. *Science*, 2001, 292, 2060
- [15] Grivas C, Li C Y, Andreakou P, et al. Single-mode tunable laser emission in the single-exciton regime from colloidal nanocrystals. *Nat Commun*, 2013, 4, 2376
- [16] Diroll B T, Dadosh T, Koschitzky A, et al. Interpreting the energy-dependent anisotropy of colloidal nanorods using ensemble and single-particle spectroscopy. *J Phys Chem C*, 2013, 117, 23928
- [17] Zhang X W, Xia J B. Linear-polarization optical property of CdSe quantum rods. *Chin J Semicond*, 2006, 27, 2094
- [18] Shabaev A, Efros A L. 1D exciton spectroscopy of semiconductor nanorods. *Nano Lett*, 2004, 4, 1821
- [19] Seo D S, Kobayashi S, Nishikawa M. Study of the pretilt angle for 5CB on rubbed polyimide films containing trifluoromethyl moiety and analysis of the surface atomic concentration of F/C(%) with an electron spectroscopy for chemical analysis. *Appl Phys Lett*, 1992, 61, 2392
- [20] Wang G W, Xiao J L. Frequency of the transition spectral line of an electron in quantum rods. *J Semicond*, 2010, 31, 092002
- [21] Xin W, Zhao Y W, Han C, et al. Magnetic field and temperature dependence of the properties of the ground state of the strong-coupling bound magnetopolaron in quantum rods with hydrogenic impurity. *J Semicond*, 2013, 34, 052001
- [22] Cunningham P D, Souza J B Jr, Fedin I, et al. Assessment of anisotropic semiconductor nanorod and nanoplatelet heterostructures with polarized emission for liquid crystal display technology. *ACS Nano*, 2016, 10, 5769
- [23] Pisanello F, Leménager G, Martiradonna L, et al. Single-photon sources: Non-blinking single-photon generation with anisotropic colloidal nanocrystals: Towards room-temperature, efficient, colloidal quantum sources (adv. mater. 14/2013). *Adv Mater*, 2013, 25, 1973
- [24] Diroll B T, Koschitzky A, Murray C B. Tunable optical anisotropy of seeded CdSe/CdS nanorods. *J Phys Chem Lett*, 2014, 5, 85
- [25] Baker J L, Widmer-Cooper A, Toney M F, et al. Device-scale perpendicular alignment of colloidal nanorods. *Nano Lett*, 2010, 10, 195
- [26] Pietra F, Rabouw F T, van Rhee P G, et al. Self-assembled CdSe/CdS nanorod sheets studied in the bulk suspension by magnetic alignment. *ACS Nano*, 2014, 8, 10486
- [27] Hu Z H, Fischbein M D, Querner C, et al. Electric-field-driven accumulation and alignment of CdSe and CdTe nanorods in nanoscale devices. *Nano Lett*, 2006, 6, 2585
- [28] Mohammadimasoudi M, Penninck L, Aubert T, et al. Fast and versatile deposition of aligned semiconductor nanorods by dip-coating on a substrate with interdigitated electrodes. *Opt Mater Express*, 2013, 3, 2045
- [29] Kaur S, Murali G, Manda R, et al. Functional film with electric-field-aided aligned assembly of quantum rods for potential application in liquid crystal display. *Adv Opt Mater*, 2018, 6, 1800235
- [30] Lutich A, Carbone L, Volchek S, et al. Macroscale alignment of CdSe/CdS nanorods by porous anodic alumina templates. *Phys Stat Sol (RRL)*, 2009, 3, 151
- [31] Amit Y, Faust A, Lieberman I, et al. Semiconductor nanorod layers aligned through mechanical rubbing. *Phys Status Solidi A*, 2012, 209, 235
- [32] Li L S, Alivisatos A P. Semiconductor nanorod liquid crystals and their assembly on a substrate. *Adv Mater*, 2003, 15, 408
- [33] Kim F, Kwan S, Akana J, et al. Langmuir–blodgett nanorod assembly. *J Am Chem Soc*, 2001, 123, 4360
- [34] Hasegawa M, Hirayama Y, Dertinger S. Polarized fluorescent emission from aligned electrospun nanofiber sheets containing

- semiconductor nanorods. *Appl Phys Lett*, 2015, 106, 051103
- [35] Du T, Schneider J, Srivastava A K, et al. Combination of photoinduced alignment and self-assembly to realize polarized emission from ordered semiconductor nanorods. *ACS Nano*, 2015, 9, 11049
- [36] Schneider J, Zhang W L, Srivastava A K, et al. Photoinduced micropattern alignment of semiconductor nanorods with polarized emission in a liquid crystal polymer matrix. *Nano Lett*, 2017, 17, 3133
- [37] Srivastava A K, Zhang W L, Schneider J, et al. Photoaligned nanorod enhancement films with polarized emission for liquid-crystal-display applications. *Adv Mater*, 2017, 29, 1701091
- [38] Zhang W L, Schneider J, Chigrinov V G, et al. Optically addressable photoaligned semiconductor nanorods in thin liquid crystal films for display applications. *Adv Opt Mater*, 2018, 6, 1800250
- [39] Dudka T, Zhang W L, Schneider J, et al. Formulation of a composite system of liquid crystals and light-emitting semiconductor quantum rods: From assemblies in solution to photoaligned films. *Adv Mater Technol*, 2019, 4, 1900695
- [40] Gupta S K, Prodanov M F, Zhang W L, et al. Inkjet-printed aligned quantum rod enhancement films for their application in liquid crystal displays. *Nanoscale*, 2019, 11, 20837
- [41] Kang C B, Zhou Z C, Halpert J E, et al. Inkjet printed patterned bank structure with encapsulated perovskite colour filters for modern display. *Nanoscale*, 2022, 14, 8060
- [42] Zhang W L, Prodanov M F, Schneider J, et al. Ligand shell engineering to achieve optimal photoalignment of semiconductor quantum rods for liquid crystal displays. *Adv Funct Mater*, 2019, 29, 1805094
- [43] Prodanov M F, Kang C B, Gupta S K, et al. Unidirectionally aligned bright quantum rods films, using T-shape ligands, for LCD application. *Nano Res*, 2022, 15, 5392
- [44] Prodanov M F, Gupta S K, Kang C B, et al. Thermally stable quantum rods, covering full visible range for display and lighting application. *Small*, 2021, 17, e2004487
- [45] Kang C B, Prodanov M F, Gao Y Y, et al. Quantum-rod on-chip LEDs for display backlights with efficacy of 149lmW^{-1} : A step toward 200lmW^{-1} . *Adv Mater*, 2021, 33, 2104685
- [46] Srivastava A K, Hu W, Chigrinov V G, et al. Fast switchable grating based on orthogonal photo alignments of ferroelectric liquid crystals. *Appl Phys Lett*, 2012, 101, 031112
- [47] Chigrinov V, Pikin S, Verevochnikov A, et al. Diffusion model of photoaligning in azo-dye layers. *Phys Rev E*, 2004, 69, 061713
- [48] Shteyner E A, Srivastava A K, Chigrinov V G, et al. Submicron-scale liquid crystal photo-alignment. *Soft Matter*, 2013, 9, 5160
- [49] Dammann H, Görtler K. High-efficiency in-line multiple imaging by means of multiple phase holograms. *Opt Commun*, 1971, 3, 312
- [50] Tam A M, Fan F, Du T, et al. Bifocal optical-vortex lens with sorting of the generated nonseparable spin-orbital angular-momentum states. *Phys Rev Applied*, 2017, 7, 034010



Wanlong Zhang received his Ph.D. degree in 2019 from the Hong Kong University of Science and Technology. Now he is an assistant professor in Shenzhen University. His research interests include liquid crystal photoalignment, liquid crystal photonics, liquid crystal on silicon, optical neural network and optical field manipulation.



Abhishek K. Srivastava is an Associate Professor and Associate Director of Centre for Display Research, at the Hong Kong University of Science and Technology. He received his Ph.D. degree in 2009 from the University of Lucknow, India. He is the Editor-in-Chief of Journal of the Society for Information Displays. He is a senior member of the Society for Information Display (SID), United States, and a member of IEEE. His current research interests include photo-alignment technology, nanomaterials, and fast liquid crystals for advanced displays and photonic devices. In 2014, he received the ILCS Early-Career Award: The Michi Nakata Prize for his early career efforts in the field of ferroelectric liquid crystals and photo-alignment. In 2018, he received the best I-zone display prototype of the year award from the SID display week for the ferroelectric liquid crystal displays. In the same year, he received the LG Bronze award from the Korean information display society for the newly developed quantum rod enhancement film. To date, he has published 228 research papers and holds 44 patents/patent applications.